Thermomagnetic studies on the Heisenberg antiferromagnet $Cs_2FeCl_5 \cdot H_2O$

J. A. Puértolas and R. Navarro
Departamento de Fisica, Escuela Tecnica Superior de Ingenieros Industriales, Universidad de Zaragoza, Spain

F. Palacio, J. Bartolomé, and D. González
Departamento de Fisica Fundamental, Facultad de Ciencias, Universidad de Zaragoza, Spain

Richard L. Carlin
Department of Chemistry, University of Illinois at Chicago, Chicago, Illinois 60680
(Received 6 July 1981; revised manuscript received 28 December 1981)

The specific heat of antiferromagnetic $Cs_2FeCl_5 \cdot H_2O$ between 1 and 30 K is reported. The long-range ordering temperature is 6.54 ± 0.02 K. A careful examination of the possible superexchange paths, and the analyses of the magnetic heat capacity and of previously reported susceptibility data in terms of spin-wave theory and high-temperature series expansions, show that the magnetic lattice effectively has a three-dimensional character, its behavior lying in between that of a simple cubic and a body centered cubic Heisenberg $S = \frac{5}{2}$ antiferromagnet (with $J/k_B = -0.29$ and -0.19 K, respectively). Furthermore, an estimate of the ratio between the several exchange interactions occurring is obtained by means of lattice crossover theory.

I. INTRODUCTION

There has been recent interest in the study of the magnetic properties of compounds of the series $A_2FeCl_5 \cdot H_2O$ where A = Cs, Rb, K, or NH_4. Thus, for A = Cs and Rb, zero-field magnetic susceptibilities and the H-T phase diagram have been reported,[1-4] while for A = K and NH_4 there exist measurements of the zero-field magnetic susceptibilities and heat capacities.[5] The magnetic phase diagram has also been investigated for A = K.[4] Moreover, some heat-capacity work has been done on the Cs and Rb compounds.[6] Several analogous bromides have also been reported.[7]

Interest in these compounds arises from the fact that they provide good examples of the Heisenberg $S = \frac{5}{2}$ antiferromagnet. Furthermore, few magnetic studies exist to date on compounds of the Fe(III) ion. Lastly, the magnetic order occurs at temperatures low enough to permit the study of the magnetic contribution to the heat capacity.

Another point of interest concerns the apparent absence of a correlation between the crystal structures and magnetic properties. In the first place, all the compounds are orthorhombic, although the space group for A = Rb, K, and NH_4 is *Pnma*[3,8,9] and for Cs is *Cmcm*.[3] On the other hand, while two members of the series seem to behave as three-dimensional magnetic systems (A = Cs,K),[2,5] the others (A = Rb, NH_4) present evidence for significant lower-dimensional magnetic order.[5,6] It is clear that the A cations do not play a direct role in the exchange interactions,[10] however they apparently modify slightly the distances and angles between molecular units, favoring, in each case, one or another magnetic dimensionality. In this paper we shall restrict the study to $Cs_2FeCl_5 \cdot H_2O$, leaving for a further paper the analysis of the $Rb_2FeCl_5 \cdot H_2O$ data and the comparative study of the members of this series.

From the analysis of the susceptibility in the paramagnetic region, the Cs compound exhibits a behavior close to that expected for a simple cubic lattice.[2] However, discrepancies with this model appeared for $T < 1.24T_c$. The susceptibility of this compound has also been interpreted in terms of a magnetic linear chain with a substantial interaction[1,3,6] between the chains. In order to investigate this point further, we present here a careful study and analysis of the magnetic heat capacity of $Cs_2FeCl_5 \cdot H_2O$, as well as a reanalysis of the existing zero-field magnetic susceptibility data in both the antiferromagnetic and the paramagnetic regions. These analyses, together with a study of the structural characteristics of the compound, allow us to determine the effective magnetic dimensionality and the relative strengths of the various superexchange interactions.

The plan of the paper is as follows. First, we study the structural characteristics and superexchange paths in $Cs_2FeCl_5 \cdot H_2O$, then we report and analyze the heat-capacity measurements. Thereafter the existing magnetic susceptibility measurements are reinterpreted and, finally, in the last section we compare and summarize the results.

II. STRUCTURAL CHARACTERISTICS

The crystal structure of $Cs_2FeCl_5 \cdot H_2O$ has recently been reported.[3] As mentioned, it crystallizes in the orthorhombic space group *Cmcm*, with cell dimensions $a = 7.442(3)$ Å, $b = 17.307(7)$ Å, $c = 8.077(7)$ Å, and four molecules per unit cell. The lattice consists of discrete octahedral units in which five chlorine atoms and one water molecule surround each iron atom. The Cs atoms align parallel to the *b* axis. The octahedra show a tetragonal distortion, the shortest distance being Fe-O followed by Fe-Cl along the apical axis. In Fig. 1 a composition of two unit cells is shown; for clarity only a few of the Cs atoms have been included.

In the structure each iron atom, e.g., the one indicated with an asterisk, is surrounded in a similar way by 10 Fe neighbors, as shown in Fig. 2. Four of these atoms, Fe^{VII}, Fe^{VIII}, Fe^{IX}, and Fe^{X} are in the same *ac* plane, forming a rhombus with its center at the central iron atom, Fe^*, the diagonals of the rhombus being parallel to the *a* and *c* axes. The distances from the corners of the rhombus to the center are, respectively, 7.442 and 8.077 Å. In a plane parallel to the rhombus but displaced along the *b* axis there are found four more atoms forming a square, Fe^{I}, Fe^{II}, Fe^{III}, and Fe^{IV}, each at 7.06 Å from Fe^*. Finally Fe^*, Fe^{V}, and Fe^{VI} form a plane which lies in the *bc* plane, Fe^{V} and Fe^{VI} being at 5.84 Å from the central iron.

It is clear that direct exchange and dipole-dipole interactions may be excluded, for the shortest Fe-Fe distance is about 6 Å. It is possible, however, to distinguish four distinct superexchange interaction paths, each corresponding to one of the four distances in the groups mentioned above.

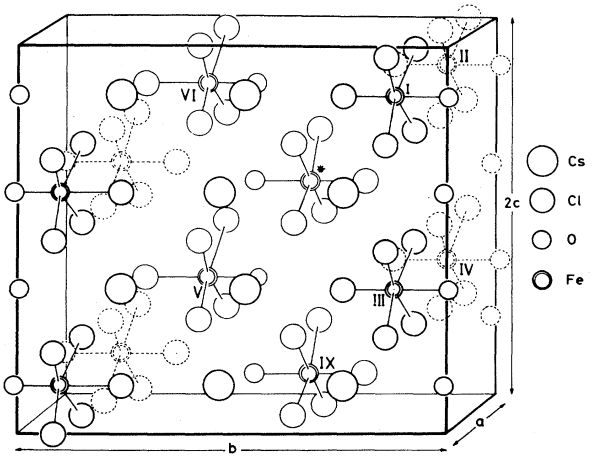

FIG. 1. Crystal structure of $Cs_2FeCl_5 \cdot H_2O$. The unit cell is doubled along the *c* axis. For clarity, only the Cs atoms in the frontal *bc* plane have been included. The differences in thickness of the atoms indicate different *bc* planes.

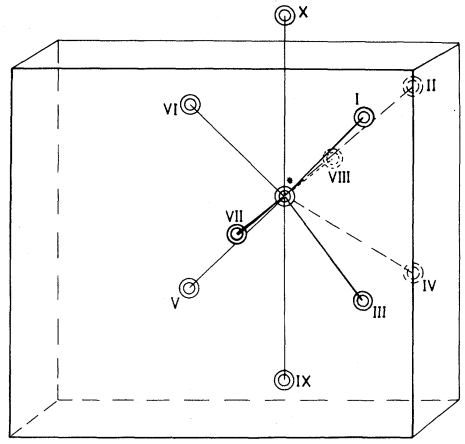

FIG. 2. Nearest ten iron neighbors around a reference Fe atom in the $Cs_2FeCl_5 \cdot H_2O$ structure.

The first path, labeled by the associated exchange interaction J_1, would go through mixed oxygen-chlorine bridges forming zig-zag chains parallel to the *c* axis. There are two identical J_1 pathways of the type Fe^*–O–Cl–Fe connecting Fe^* to Fe^{V} and Fe^{VI}, each of these occurring twice since there are two equivalent chlorine atoms per interaction. These equivalent paths are shown schematically in Fig. 3(a).

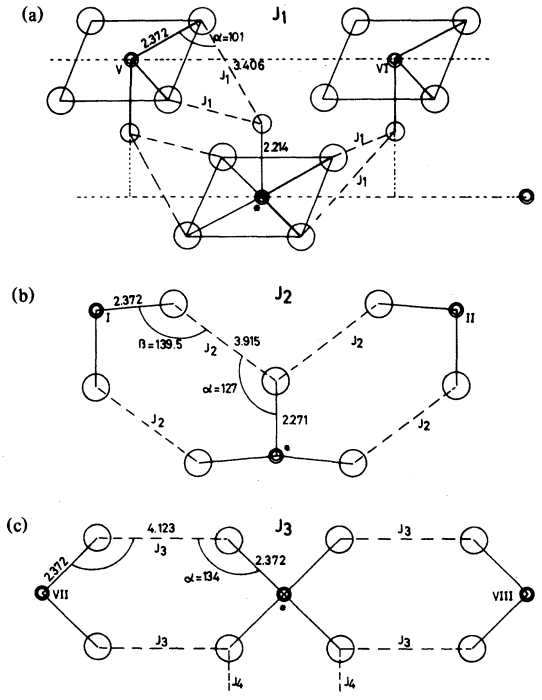

FIG. 3. (a)–(c) Superexchange interaction paths for $Cs_2FeCl_5 \cdot H_2O$. Only the relevant distances and angles have been written down. Roman numerals identify iron atoms with those shown in Fig. 2. In the top diagram, the $FeCl_4$ plane lies in the *ac* plane.

A second interaction, J_2, would connect every iron atom with the four nearest neighbors that have the apical O–Fe–Cl axis inverted with respect to one another. Therefore this interaction is transmitted through one apical Cl and another equatorial Cl atom as shown in Fig. 3(b). Again double bridges are formed, this time of the type Fe^*–Cl–Fe, connecting Fe^* to Fe^{I}, Fe^{II}, Fe^{III}, and Fe^{IV}.

There are, finally, two more interactions, J_3 and J_4, that should be considered. They would connect iron atoms through equatorial chlorines in planes parallel to the *ac* plane, as shown in Fig. 3(c). The interaction J_3 connects Fe^* to Fe^{VII} and Fe^{VIII}, the interaction J_4 connects it to Fe^{IX} and Fe^{X}.

As it is clear, not all these paths are equivalent, since the strength of exchange interactions is very sensitive to distance, the dependence for simple bridged collinear paths being of the form r^{-11}, r^{-12} or exponential.[11] In the present case we expect the distance between the two ligands (Cl–O or (Cl–Cl) to be the crucial parameter in determining the strength of the superexchange interactions. Then, J_4 should be the weakest interaction, since the Cl-Cl distance between the interacting chlorines is the largest, i.e., 4.758 Å compared with 4.123 and 3.915 Å for the corresponding Cl-Cl distances in J_3 and J_2, respectively, or when compared with the Cl-O distance of 3.406 Å in J_1. Consequently, the J_4 interaction will henceforth be neglected.

The angles between the bonds in interactions J_2 and J_3 are quite similar, for $\alpha = \alpha' = 134°$ in J_3 do not differ appreciably from $\beta' = 139°$ and $\beta = 124°$ in J_2. There is, however, a slightly larger (5%) distance between the chlorines in J_3 when compared with J_2; also the apical chlorine atom in J_2 is 5% closer to the iron atom than the equatorial ones. In accounting for all these small differences it seems reasonable to consider J_2 as somewhat larger than J_3, none of these being nevertheless negligible. Finally, the interaction J_1 has to be considered as the strongest one, since oxygen ligands provide stronger exchange than chlorine ones and because of the smaller O-Cl distances. It is therefore possible to order the interactions as $J_1 > J_2 > J_3$.

From the above analysis, we could expect to find one-dimensional magnetic behavior if $J_1 >> J_2, J_3$; however, the nature of the heat capacity excludes this possibility. If, on the other hand, J_2 or J_3 are competitive to J_1 the behavior becomes three dimensional directly, because the bonds extend three dimensionally in the lattice. As a consequence, the effective number of magnetic neighbors can be expected to be smaller than $z = 8$ (i.e., if $J_1 = J_2 = J_3$), and discrepancies with calculations for a body centered cubic lattice should be expected. Therefore, the simple cubic Heisenberg model (with spin value $S = \frac{5}{2}$), i.e., an isotropic model with six equivalent neighbors will be used below as a first attempt to fit the data. The values of the exchange constant, J, obtained will then be an average of the three interactions. In the last section of the present work the data are also compared with bcc model predictions.

III. HEAT-CAPACITY MEASUREMENTS

A. Installation

Heat-capacity measurements were performed from 1 to 30 K with an adiabatic calorimeter following the standard heat pulse technique. In the installation, the vacuum can containing the calorimetric setup is immersed in liquid ^{4}He. The relevant parts are shown schematically in Fig. 4. The liquid-helium pot *B* is thermally isolated from the main helium bath.

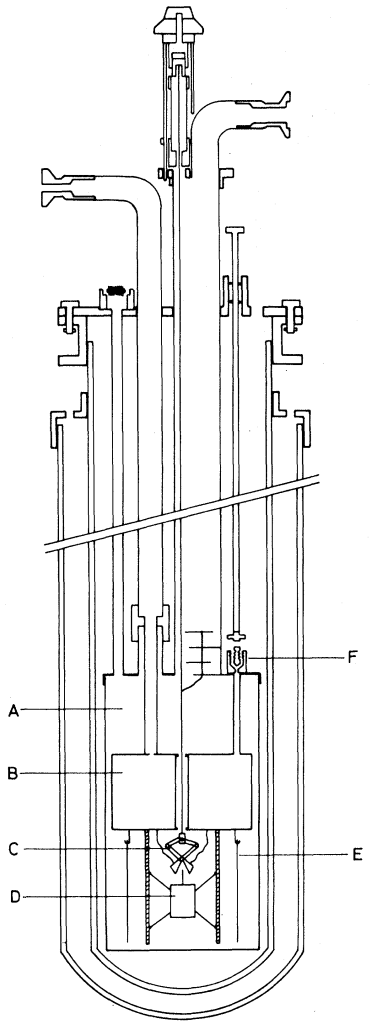

FIG. 4. Calorimeter insert: (a) vacuum chamber; (b) liquid helium pot; (c) heat switch; (d) calorimetric vessel; (e) adiabatic shield; and (f) needle valve.

By pumping on the helium in this pot through a minute hole of 0.4 mm diameter it is possible to obtain temperatures of about 1 K in the pot. The thermal contact between the calorimetric vessel D and the pot B is established with the aid of a mechanical heat switch that can be externally operated.

The installation was calibrated using a standard high-purity copper sample (99.999%) as recommended by the 1965 Calorimetry Conference. The sample was adequately treated for surface decontamination.[12]

The accuracy of our measurements was better than 1% in the temperature range from 1 to 30 K. The values $\gamma = 0.694 \pm 0.001R$ K^{-1} and $\Theta_D(0) = 341.0 \pm 0.2$ K, obtained from fitting the data to the equation $C_P/T^2 = A + BT$, where $A = \gamma/R$ and $B = 12\pi^4 R/5[\Theta_D(0)]^3$, are in good agreement with those given by the National Bureau of Standards [$\gamma = 0.695 \pm 0.005R$ K^{-1} and $\Theta_D(0) = 344.5 \pm 1.5$ K].[13]

The calorimetric vessel for powdered samples consists of a copper cylinder on which a noninductively wound heater is cemented with GE-7031 varnish. The cylinder has a stainless-steel top containing the Ge thermometer. The sample holder, made of gold-plated copper, is located in the interior of the cylinder, using Apiezon T in order to improve thermal contact. Thermal contact within the sample holder itself is optimized by alternating gold-plated copper plates with the powdered sample and pressing the whole ensemble. Electrical wires extending from the calorimetric vessel are thermally anchored to the adiabatic shield. With a good control of the temperature of the adiabatic shield it is possible to achieve sufficient quasiadiabaticity in the measurements. A more detailed description of the installation and calibration can be found in Refs. 14 and 15.

B. Measurements

The sample of $Cs_2FeCl_5 \cdot H_2O$ was prepared by powdering crystals grown by evaporation from aqueous solution.

Although some heat-capacity measurements of $Cs_2FeCl_5 \cdot H_2O$ have previously been reported,[6] these data proved to be unsuitable for analysis owing to the following reasons: (a) the lattice contribution cannot be satisfactorily evaluated because of the large scatter in the points, being 5% to 10% for $T > 15$ K, and (b) the lowest temperature of the measurements was 2.3 K, which is too high to permit a reliable study of the ordered region with spin-wave theory. We decided, therefore, to extend the temperature range of the measurements down to 1 K, and furthermore obtained a much higher accuracy of the measurements (to better than 1%). Moreover, after our measurements were finished we observed a systematic discrepancy with O'Connor's data, his molar C_P values being 15–20% higher than ours. We have therefore disregarded O'Connor's measurements in the analyses below.

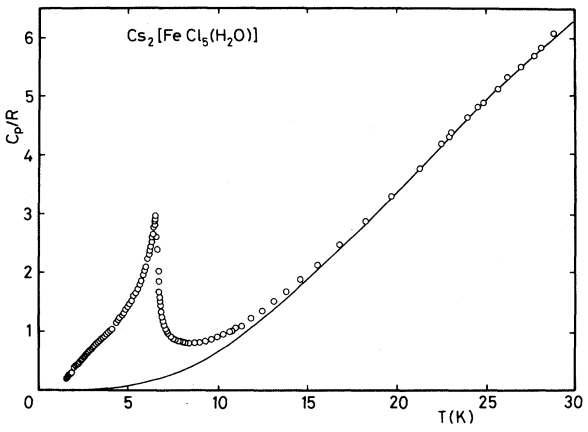

FIG. 5. Experimental heat-capacity data (circles) and calculated lattice contribution (continuous line) for $Cs_2FeCl_5 \cdot H_2O$.

Our own results for the heat capacity (with the addenda subtracted) are shown in Fig. 5 and are tabulated in Table I. The magnetic anomaly is found to peak at $T_c = 6.54 \pm 0.02$ K in good agreement with the $T_c = 6.43$ K deduced from the susceptibility.

TABLE I. Reduced heat capacity of $Cs_2FeCl_5 \cdot H_2O$.

T (K)	C_P/R	T (K)	C_P/R	T (K)	C_P/R
Series I		Series II			
4.531	1.218	2.479	0.510	6.423	2.754
4.785	1.280	2.530	0.537	6.455	2.796
5.068	1.407	2.587	0.558	6.487	2.858
5.430	1.600	2.665	0.584	6.514	2.973
5.723	1.766	2.755	0.617	6.538	2.899
5.947	1.930	2.858	0.650	6.561	2.907

TABLE I (*Continued*).

T (K)	C_P/R	T (K)	C_P/R	T (K)	C_P/R
	Series I		Series II		
6.110	2.067	2.979	0.677	6.585	2.811
6.245	2.103	3.106	0.727	6.612	2.614
6.366	2.252	3.221	0.762	6.641	2.398
6.470	2.477	3.315	0.792	6.675	2.023
6.562	2.574	3.406	0.821	6.702	1.851
6.634	4.277	3.495	0.850	6.722	1.670
6.754	1.547	3.592	0.878	6.744	1.575
6.894	1.271	3.694	0.913	6.768	1.510
7.086	1.131	3.793	0.939	6.793	1.434
7.295	0.961	3.890	0.970	6.825	1.330
7.515	0.895	3.984	1.006	6.867	1.242
7.994	0.760	4.071	1.033	6.920	1.165
8.233	0.797	4.171	1.042	6.988	1.100
8.465	0.780	4.468	1.179	7.068	1.037
8.727	0.815	4.569	1.222	7.154	0.991
9.044	0.819	4.671	1.255	7.263	0.951
9.370	0.852	4.777	1.303	7.397	0.903
10.79	1.011	4.881	1.354	7.534	0.874
11.32	1.090	4.984	1.399	7.686	0.850
11.86	1.214	5.095	1.449	7.858	0.832
12.46	1.344	5.212	1.517	8.033	0.817
13.11	1.502	5.328	1.596	8.225	0.800
13.80	1.865	5.440	1.642	8.456	0.801
14.61	1.873	5.545	1.722	8.728	0.804
15.57	2.124	5.647	1.794	8.999	0.815
16.79	2.470	5.743	1.864	9.311	0.837
18.26	2.881	5.831	1.958	9.657	0.875
19.72	3.312	5.925	2.034	9.985	0.911
21.27	3.775	6.015	2.102	10.32	0.958
22.96	4.312	6.100	2.241	10.68	0.999
24.92	4.899	6.183	2.311	11.03	1.066
27.01	5.516	6.243	2.381	22.50	4.199
28.87	6.102	6.284	2.443	23.98	4.651
30.60	6.473	6.322	2.518	25.71	5.137
32.56	6.980	6.359	2.606	27.78	5.707
		6.392	2.658	30.51	6.502
	Series III(a)			Series III(b)	
1.523	0.177	2.195	0.421	23.10	4.397
1.579	0.181	2.265	0.451	24.59	4.829
1.632	0.209	2.345	0.475	26.27	5.344
1.691	0.237	2.423	0.504	28.14	5.844
1.763	0.265	2.501	0.537	30.12	6.411
1.846	0.290	2.583	0.562	32.37	6.796
1.924	0.353	2.670	0.590	34.84	7.567
1.998	0.357	2.768	0.620		
2.063	0.405	2.880	0.666		
2.129	0.395	3.002	0.704		

IV. ANALYSIS OF THE MEASUREMENTS

A. Lattice contribution

In order to study the magnetic contribution to the heat capacity, the lattice contribution has to be accounted for. An obvious method is to apply a corresponding states analysis, using the heat-capacity data of a diamagnetic isomorphous salt.[16] Unfortunately, this is not possible in the case of $Cs_2FeCl_5 \cdot H_2O$ since no isomorphous diamagnet is known. We have therefore evaluated the phonon contribution following a different procedure.

The lattice heat capacity of many insulators has been fitted to an asymptotically convergent series[17]

$$C_L = BT^3 + CT^5 + \cdots .$$

Besides, the magnetic contribution for temperatures sufficiently above T_c adds a new term AT^{-2} to account for the measured heat capacity. In order to determine the constants A,B,C, etc., we have followed a least-squares fitting procedure with several constraints. First, the deviation of the calculated points from the experimental ones had to be less than 1% in the largest possible temperature interval above T_c. Secondly, the entropy of the magnetic contribution, evaluated (by integration of the specific-heat curve) after subtracting the lattice contribution from the total heat capacity, must have a value as close as possible to the theoretical one for $S=\frac{5}{2}$, namely, $\Delta S/R = \ln(2S+1) = 1.79$. Finally, the coefficients so obtained should not be too sensitive to the temperature interval chosen for the fitting. In Table II we give the coefficients of the optimum polynomial so obtained; the coefficients are valid in the temperature range $0 < T < 30$ K. The lattice contribution thus calculated is shown in Fig. 5 as a continuous line.

It is worthwhile to remark that if the empirical value of A is set equal to the coefficient of the T^{-2} term in the high-temperature series expansion for a simple cubic lattice, that is, $\frac{2}{3}z[S(S+1)]^2(J/k_B)^2$ with $z=6$ and $S=\frac{5}{2}$, we obtain $J/k_B = -0.29 \pm 0.01$ K, in good agreement with the value $J/k_B = -0.31$ K obtained from the fit of the susceptibility.[2] This is also a good test for the procedure followed in the evaluation of the lattice contribution.

TABLE II. Fitted coefficients for the polynomial $C_P = AT^{-2} + BT^3 + CT^5 + DT^7 + ET^9$.

$A =$	$0.270\,320\,355\,9E+2$
$B =$	$0.761\,993\,318\,5E-3$
$C =$	$-0.115\,901\,892\,5E-5$
$D =$	$0.853\,629\,140\,7E-9$
$E =$	$-0.238\,055\,257\,4E-12$

B. Magnetic contribution

The magnetic contribution to the heat capacity can now be evaluated by subtracting the lattice heat capacity from the total measured specific heat as shown in Fig. 6. The entropy change for this contribution, $\Delta S/R = 1.69$, agrees within 5% with the theoretical value. As mentioned previously, the nature of the peak precludes the assignment of significant one-dimensional magnetic ordering, for which one expects broad Schottky-type specific-heat curves. From the total magnetic energy $\Delta E/R = 9.189$ we can obtain further information with the approximate relation $\Delta E/R = zS^2(J/k_B)$. Thus, for $z=6$ we calculate $|J/k_B| = 0.25 \pm 0.01$ K.

In order to fit the experimental results in detail to the theoretical predictions and evaluate the exchange interaction, two temperature regions were considered. In the ordered region, at temperatures well below T_c, we have applied the theory of free spin waves[18] for a simple cubic (sc) Heisenberg antiferromagnet with $S=\frac{5}{2}$ and an anisotropy constant[2] $\alpha = 1.2 \times 10^{-2}$. Satisfactory agreement with the experimental points could be obtained for $J/k_B = -0.27 \pm 0.01$ K, as shown by curve "a" in Fig. 6. Neither kinematic nor dynamic corrections have been considered in these calculations.

In the paramagnetic region, at temperatures well above T_c, the high-temperature series expansion for the specific heat of the same model[19] was found to fit

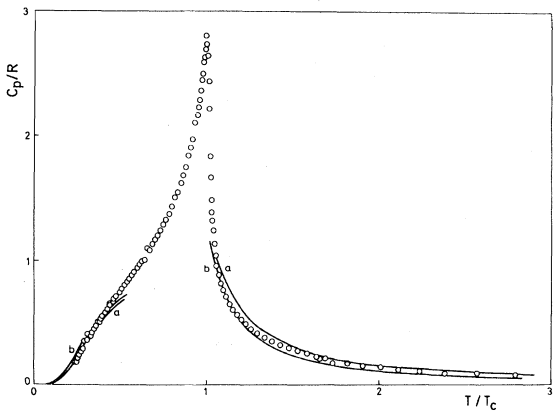

FIG. 6. The magnetic contribution to the heat capacity. Solid lines are theoretical predictions obtained from spin-wave theory and from high-temperature series expansions for the Heisenberg $S=\frac{5}{2}$ antiferromagnet as described in the text. Curves labeled "a" and "b" refer to the sc and bcc lattices, respectively.

the experimental heat-capacity points for $J/k_B = -0.255 \pm 0.005$ K. We remark that we have used the Padé approximants technique[20] to obtain an extrapolation to temperatures lower than the apparent validity of the high-temperature series. Details of the calculations may be found in Ref. 21. Finally, we may determine J/k_B from the prediction for the normalized critical temperature obtaining $J/k_B = -0.263 \pm 0.001$, which compares satisfactorily with the above determinations.

V. ANALYSIS OF SUSCEPTIBILITY DATA

Two sets of single-crystal magnetic susceptibility measurements on $Cs_2FeCl_5 \cdot H_2O$ are available in the literature.[3,6] Previous analysis of the data in the paramagnetic region had shown[2] that this compound apparently behaves as a simple-cubic Heisenberg system, with exchange interaction $J/k_B = -0.310 \pm 0.005$ K. We have reanalyzed the data measured in Chicago[6] according to the following methods.

A theoretical estimate of the antiferromagnetic critical temperature was obtained by an analysis of the singularity of the staggered susceptibility series[22] for the three-dimensional sc and bcc Heisenberg lattices with $S = \frac{5}{2}$ and equivalent neighbors. In order to do this, the usual methods of analysis for the ferromagnetic singularity were applied,[23] adopting a value for the critical exponent of $\gamma = 1.43$, as has previously been found for $S = \frac{1}{2}$ in the three-dimensional lattices.[24] Moreover, the height and the position of the maximum occurring in the antiferromagnetic susceptibility above T_c were calculated using extrapolation techniques of the high-temperature series[19,25] based on Padé approximants as described elsewhere.[26] The results found for the critical parameters are summarized in Table III in dimensionless units. From these theoretical predictions and by substituting the experimental values $T_c = 6.43$ K, (as calculated from $(\partial\chi_{\parallel}/\partial T)_{max}$), $T(\chi_{max}) = 7.20$ K and $\chi_{max} = 0.207$ emu/mol, we obtain for the sc lattice a value of $|J|/k_B = 0.259$, 0.275, and 0.290 K, respectively.

TABLE III. Antiferromagnetic critical temperature (T_c), height (χ_{max}) and position on the temperature axis $T(\chi_{max})$ of the susceptibility maximum for the Heisenberg antiferromagnet with $S = \frac{5}{2}$ on the sc and bcc lattices.

	sc	bcc
$k_B T_c/\|J\|S(S+1)$	2.84	4.04
$k_B T(\chi_{max})/\|J\|S(S+1)$	3.07 ± 0.08	4.18 ± 0.09
$\chi_{max}\|J\|/Ng^2\mu_B^2$	0.0394	0.0301

For the analysis of the data in the ordered region we have applied spin-wave theory,[18,21,26] analogous to that used for the analysis of the heat-capacity data. However, in this case the dynamic interactions between the spin waves have been included. The reason is that in the case of the susceptibility such a correction to the free spin-wave prediction is already substantial at very low temperatures and thus has to be accounted for in the fitting. For the heat capacity, however, the correction is only minor in the (temperature) range of validity of the spin-wave theory, so that we have discarded it in the above.

For a simple cubic lattice, and with α as given in the literature,[2] we so obtain $J/k_B = -0.31$ K from $\chi_{\perp}$, and $J/k_B = -0.29$ K from $\chi_{\parallel}$, where the fitting procedure was limited up to $T = 3$ K since above this temperature the use of such a theory would be unrealistic. In Fig. 7 the agreement of the fit with the experimental points is shown (curves "a" of $\chi_{\parallel}$ and $\chi_{\perp}$) on a reduced scale. Such a scale is most useful for comparative purposes. Indeed, in the same figure we have plotted the molecular field prediction for $\chi_{\perp}$, and the experimental data for $\chi_{\perp}$ of $RbMnF_3$,[27] one of the best examples of the sc Heisenberg antiferromagnet with $S = \frac{5}{2}$. The differences observed in the maxima for both sets of experimental data points are attributed to deviations from this ideal model present in the compound $Cs_2FeCl_5 \cdot H_2O$.

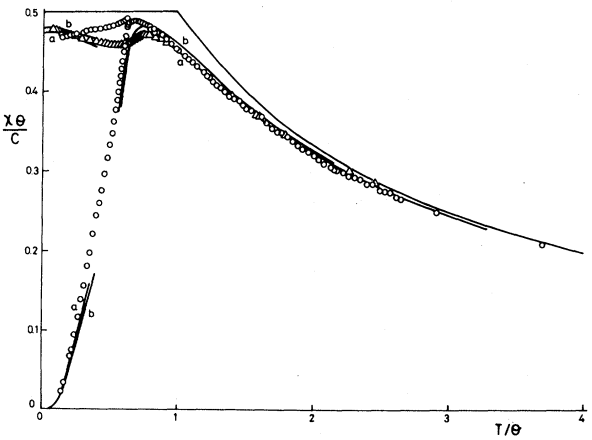

FIG. 7. Parallel and perpendicular susceptibilities of $Cs_2FeCl_5 \cdot H_2O$ on a reduced scale. Solid lines are theoretical predictions obtained from spin-wave theory and from high-temperature series expansions for the Heisenberg $S = \frac{5}{2}$ antiferromagnet. Curves "a" and "b" again refer to the sc and bcc lattice, respectively. Susceptibility data for $RbMnF_3$(Δ) (Ref. 23) as well as molecular-field predictions (line at $\chi\Theta/C = 0.5$) have been included for comparison.

VI. DISCUSSION

In the center column of Table IV, we have compiled the values for J/k_B as calculated from the various fits of the experimental data to predictions based upon the Heisenberg sc, $S=\frac{5}{2}$ antiferromagnet. Agreement with the theory is rather good although not complete. Some discrepancies were however to be expected when the ideal simple cubic lattice was taken as the theoretical model. For, as described above, we have to take into account the three different interactions J_1, J_2, and J_3, which couple a given reference ion to a total of eight magnetic nearest neighbors. Therefore, fits of the experimental data to bcc Heisenberg $S=\frac{5}{2}$ model predictions ($z=8$) have likewise been made and the results are also collected in Table IV. The corresponding predictions are also shown in Figs. 5 and 6 as the curves "b." It is clear that the agreement is of about the same quality as when the sc lattice is considered. Similar results are found when we examine the distribution of energy and entropy above and below T_c. These values are listed in Table V and compared with the theoretical predictions for antiferromagnetic Heisenberg, sc and bcc models with $S=\infty$, for, to our knowledge, there are no such calculations for $S=\frac{5}{2}$. In order to make a comparison with another $S=\frac{5}{2}$ three-dimensional Heisenberg system we have included our data on sc NH_4MnF_3 in Table V.

Although the entropy parameter has a value closer to that calculated for the sc lattice, the energy distribution parameter above T_c is more or less in between the expectation for the sc and bcc lattices; in any case the behavior is clearly three dimensional.

The ambiguity of the data analysis in this respect could be due to the inequivalency of the three interactions, or even when one would have $J_3 \sim 0$, to the difference between J_1 and J_2. It is clear that in the latter case the effective number of magnetic neighbors would be even smaller than $z=6$. As a matter of fact, if we use the first high-temperature series coefficient A, and the experimental total magnetic energy in order to determine the number of equivalent paths, we obtain $z=4.01$. There are gross approximations involved, and also accumulative errors in this determination, but give basis for a more careful study of the inequality between J_1 and J_2 paths.

The competing exchange interactions, in our case (J_1 and J_2), may cause lattice crossover effects in the magnetic properties. From the analysis of exchange paths above, we conclude that the relevant case is the one- to three-dimensional crossover. We have elaborated the theoretical predictions for the relevant thermodynamic functions in terms of the lattice anisotropy $R=J_2/J_1$, by using the high-temperature expansions for a sc classical spin Heisenberg model.[28] The details of those calculations will appear elsewhere as a conclusive demonstration of the lower dimensional character of the magnetic lattice in the related $Rb_2FeCl_5 \cdot H_2O$ compound.[29]

By comparing the χ data to the predictions obtained for χ_{max} and T_c as a function of R, we estimate that $(\frac{1}{2})|J_1| \leq |J_2| \leq |J_1|$. The fits of the data to predictions of χ above T_c are in fact of the same quality as those with the sc or bcc model pre-

TABLE IV. Summary of $-J/k_B(K)$ values for the sc and bcc lattices.

Calculated from	Simple cubic	Body centered cubic
χ (high-temperature series)	0.310 ± 0.005	0.235
χ_{max}	0.290 ± 0.003	0.221 ± 0.002
T_c [from $(\partial\chi/\partial T)_{max}$]	0.259 ± 0.002	0.188 ± 0.001
T (χ_{max})	0.275 ± 0.001	0.198
$\chi_\perp$ (spin waves)	0.310 ± 0.003	0.210 ± 0.003
$\chi_\parallel$ (spin waves)	0.293 ± 0.005	0.236 ± 0.002
T_c (from C_P)	0.263 ± 0.001	0.185 ± 0.001
C_P (spin waves)	0.270 ± 0.01	0.195 ± 0.001
C_P (high-temperature series)	0.255 ± 0.005	0.184 ± 0.005
C_P (T^{-2} coefficient)	0.29 ± 0.01	0.216
C_P (total magnetic energy)	0.25 ± 0.01	0.18 ± 0.01
H_e (exchange field)	0.342	0.257

TABLE V. Entropy and energy parameters of $Cs_2FeCl_5 \cdot H_2O$ as compared with sc and bcc ($S = \infty$) theoretical predictions and sc NH_4MnF_3 experimental results.

Parameter	$Cs_2FeCl_5 \cdot H_2O$	sc($S = \infty$)	bcc($S = \infty$)	NH_4MnF_3 (Ref. 14)
$(S_\infty - S_c)/R$	0.397	0.42	0.338	0.40
$(E_c - E_0)/RT_c$	0.818	· · ·	· · ·	0.834
$(E_\infty - E_c)/RT_c$	0.587	0.69	0.533	0.685
$(E - E_0)/RT_c$	1.405	· · ·	· · ·	1.519
J/k_B(K)	−0.29	· · ·	· · ·	−3.02

dictions. Thus, the ratio of the three interactions J_1, J_2, and J_3 cannot be obtained with precision. Also, from the comparison of the exchange paths it seems further likely that J_3 is not negligible when compared to J_2. What is certain, however is the predominant three-dimensional character of the magnetic ordering.

ACKNOWLEDGMENTS

R.L.C. would like to thank the Instituto de Ciencias de la Educacion and Vice-rectorado de Extension Universitaria, Universidad de Zaragoza, for travel funds which facilitated the preparation of this manuscript. The Juan March Foundation supported the contribution by the group at Zaragoza, and the National Science Foundation, Solid State Chemistry Program, under Grant No. DMR-7906119 supported the contribution in Chicago. We should also like to thank D. W. Osborne and H. Flotow for the sample of high-purity copper used in the calibrations. The referee provided his usual sagacious comments, and we wish to express our gratitude to him.

[1]R. L. Carlin, S. N. Bhatia, and C. J. O'Connor, J. Am. Chem. Soc. 99, 7728 (1977).
[2]A. Paduan Filho, F. Palacio, and R. L. Carlin, J. Phys. (Paris) 39, L279 (1978).
[3]C. J. O'Connor, B. S. Deaver, and E. Sinn, J. Chem. Phys. 70, 5161 (1979); J. E. Greedan, D. C. Hewitt, R. Faggiani, and I. D. Brown, Acta Crystallogr. Sect. B 36, 1927 (1980).
[4]F. Palacio, A. Paduan Filho, and R. L. Carlin, Phys. Rev. B 21, 296 (1980).
[5]J. N. McElearney and S. Merchant, Inorg. Chem. 17, 1203 (1978).
[6]C. J. O'Connor, thesis (University of Illinois at Chicago Circle, 1976) (unpublished).
[7]R. L. Carlin and C. J. O'Connor, Chem. Phys. Lett. 78, 528 (1981).
[8]I. Lindqvist, Ark. Kemi, Mineral. Geol. 24, 1 (1947); B. N. Figgis, C. L. Raston, R. P. Sharma, and A. H. White, Aust. J. Chem. 31, 2717 (1978).
[9]A. Bellanca, Period. Mineral. 17, 59 (1948).
[10]P. W. Anderson, in *Magnetism,* edited by G. T. Rado and H. Suhl (Academic, New York, 1963), Vol. 1.
[11]L. J. de Jongh and R. Block, Physica B 79, 568 (1975).
[12]D. W. Osborne, H. Flotow, and F. Schreiner, Rev. Sci. Instrum. 38, 159 (1967).
[13]G. T. Furukawa, W. G. Saba, and M. L. Reilly, Nat. Stand. Ref. Data Ser., Nat. Bur. Stand. 18 (1968).
[14]J. A. Puértolas, thesis (Universidad de Zaragoza, 1980) (unpublished).
[15]R. Burriel, thesis (Universidad de Zaragoza, 1979) (unpublished).
[16]J. W. Stout and E. Catalano, J. Chem. Phys. 23, 2013 (1955).
[17]T. H. K. Barron and J. A. Morrison, Can. J. Phys. 35, 799 (1957).
[18]F. Keffer, in *Encyclopedia of Physics,* edited by H. P. J. Wijn (Springer-Verlag, New York, 1967), Vol. XVIII.
[19]G. S. Rushbrooke and P. J. Wood, Mol. Phys. 1, 257 (1958).
[20]D. L. Hunter and G. A. Baker, Jr., Phys. Rev. B 7, 3346 (1973).
[21]R. Navarro, thesis (Universidad de Zaragoza, 1976) (unpublished).
[22]G. S. Rushbrooke and P. J. Wood, Mol. Phys. 6, 409 (1963).
[23]G. A. Baker, Jr., H. E. Gilbert, J. Eve, and G. S. Rushbrooke, Phys. Rev. 164, 800 (1967).
[24]G. S. Rushbrooke, G. A. Baker, Jr., and P. J. Wood, in *Phase Transitions and Critical Phenomena,* edited by C. Domb and M. S. Green (Academic, New York, 1974), Vol. 3.
[25]P. L. Stephenson, K. Pirnie, P. J. Wood, and J. Eve, Phys. Lett. A 27, 2 (1961).
[26]R. Navarro, J. J. Smit, L. J. de Jongh, W. J. Crama, and D. J. W. Ijdo, Physica 83B, 97 (1976).
[27]L. J. de Jongh and D. J. Breed, Solid. State Commun. 15, 1061 (1974).
[28]D. N. Lambeth and H. E. Stanley, Phys. Rev. B 12, 5302 (1975).
[29]J. A. Puértolas, R. Navarro, F. Palacio, J. Bartolomé, D. Gonzaléz, and R. L. Carlin (unpublished).